Synthesis and Assessment of Glycosaminoglycan Priming Activity of Cluster-xylosides for Potential Use as Proteoglycan Mimetics

Vy M. Tran,[†] Thao K. N. Nguyen,[†] Venkataswamy Sorna,[‡] Duraikkannu Loganathan,*,[‡] and Balagurunathan Kuberan*,[†,§]

Departments of [†]Bioengineering and Medicinal Chemistry and [§]Interdepartmental Program in Neuroscience, University of Utah, Salt Lake City, Utah 84112, United States

[‡]Department of Chemistry, Indian Institute of Technology, Madras, Chennai 600 036, India

Ⓢ Supporting Information

ABSTRACT: One of the distinct structural features of many proteoglycans (PGs) is the presence of two or more glycosaminoglycan (GAG) side chains covalently linked to a core protein. Previous studies have shown that the synergistic biological activity of multiple GAG chains, as found in the majority of PGs, cannot be accomplished by the sum of the activities of individual GAG chains. To delineate the biological significance of GAG valency, a number of cluster-xylosides carrying two, three, or four xylose residues on the same scaffold were synthesized using click chemistry. Assessment of cluster-xylosides for their GAG chain priming activity in a cellular system revealed that these cluster-xylosides prime multiple GAG chains per scaffold. Multivalent GAG chains, produced by cluster-xylosides, can better mimic PGs as they carry two or more GAG chains attached to a core protein and therefore can be used as molecular probes to examine the biological significance of GAG multivalency in model organisms.
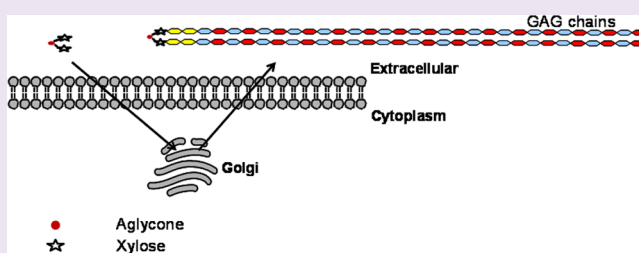
Proteoglycans (PGs) are the most ubiquitous glycoconjugates found on cell surfaces and in the extracellular matrix.[1] These highly charged, complex PGs regulate various molecular, cellular, pathological, and physiological events through binding to a wide array of proteins.[2,3] The distinct structural feature of all PGs, with the exception of a few PGs, is the substitution of a core protein with multiple glycosaminoglycan (GAG) chains such as heparan sulfate (HS), chondroitin sulfate (CS), and/or dermatan sulfate (DS) (Figure 1).[1]

GAG attachment sites are highly conserved among various PGs in several mammals.[4,5] This implies that multiple GAG chains are required for optimal biological functionality of PGs in various species. Single GAG chains can perhaps not provide the same functionality that multiple GAG chains can. Only a few studies have examined the biological significance of GAG multivalency.[4,6] The cell surface PGs from simple and stratified epithelium are shown to be polymorphic due mostly to variability in both the number of GAG chains attached to the core protein and GAG size.[7] The variable chain valency is suggested to facilitate the distinct adhesive requirements of these two epithelial cell types.

Xylosylation of certain serine residues of the core proteins, a rate-limiting first step in the assembly of PGs, is catalyzed by xylosyltransferases.[8−10] It is known that xylosides can function as GAG chain initiators without a core protein provided that xylosides carry a hydrophobic group.[11−15] We have previously shown that click-xylosides prime a diverse array of GAG chains and suggested the presence of GAGOSOMES, distinct macromolecular enzyme complexes that regulate the combinatorial biosynthesis of complex GAG chains.[16,17] Several earlier studies have rigorously utilized synthetic mono-xylosides to further our understanding of the role of endogenous PGs in model organisms and also to elucidate the elusive biosynthetic mechanism. Only one study has examined synthetic bis-xylosides, which carry two xylose residues per molecular scaffold, for their priming activity.[18] These synthetic bis-xylosides carry very labile *O*-glycosidic linkage. Given the importance of multiple GAG chains for cooperative interactions with protein ligands and for optimal biological functions, there is a great deal of interest in synthesizing stable, small molecular scaffolds carrying variable number of xylose residues for biological studies. Thus, synthetic cluster-xylosides should afford molecular scaffolds with multiple GAG chains mimicking endogenous PGs to define the role of GAG glycome and GAG multivalency in various developmental and physiological processes.

In the present study, we utilized click chemistry to assemble cluster-xylosides carrying two, three, or four xylose residues. We investigated the priming activity of these cluster-xylosides in a model cellular system, pgsA-745 cell line, lacking active xylosyltransferase.[19] Furthermore, we examined whether the distance between two xylose residues in a group of bis-xylosides and the number of xylose units in cluster-xylosides can affect the priming activity, the type of GAG chains primed, their
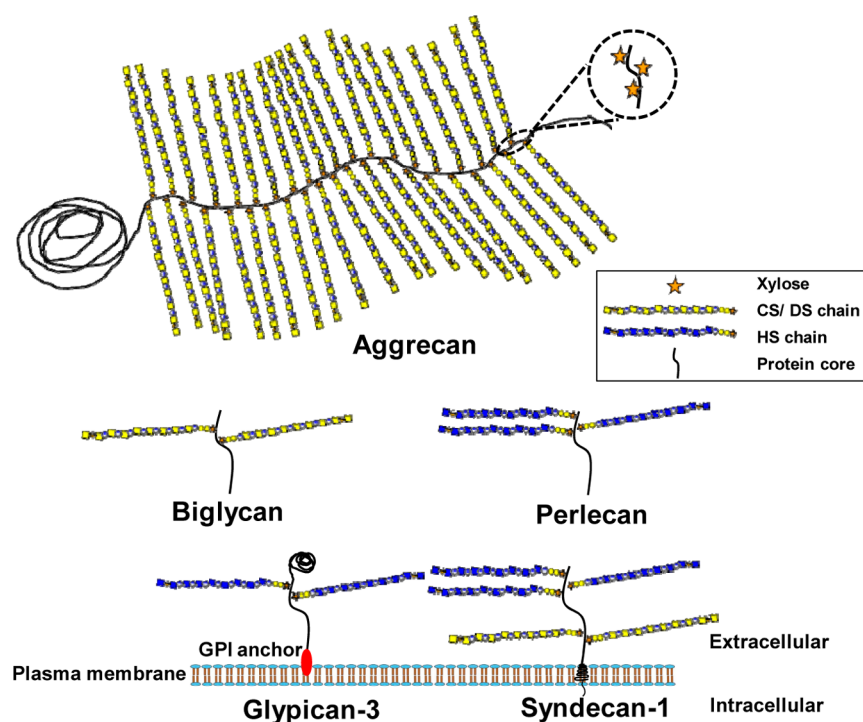
Figure 1. Schematic representation of various cell surface and ECM-bound proteoglycans. HS: heparan sulfate. CS: chondroitin sulfate. DS: dermatan sulfate.

sulfation pattern, and chain length. The results obtained in the present study provide further insights into the nature of assembly of multiple GAG chains on the synthetic scaffolds and suggest that these PG mimetics can potentially be utilized to study the functional role of GAG chain valency in biological systems.

RESULTS AND DISCUSSION

A distinct structural feature of all PGs, with the exception of a very few PGs, is that the core protein is substituted with two or more GAG chains. In addition, PGs exhibit a molecular polymorphism attributed to differences in their GAG chain valency and size.[7] The multivalent nature of PGs has been suggested to be important in regulating a wide variety of cellular processes including optimal function of syndecans in cell invasion, migration, and adhesion.[20] A recent study has exemplified the cooperative interaction of FGF-2 with heparin oligosaccharides attached to the dendrimer in potentiating FGF-2 activity.[21]

We recently demonstrated that click-xylosides carrying different aglycone moiety prime diverse GAG chains and suggested the presence of GAGOSOMES that can regulate the production of cell-specific combinatorial GAG structures with distinct sulfation pattern, size and type.[17,22−24] In this report, we examined a method to assess the effect of the distance between two GAG initiation sites on priming activity, the type of GAG produced, GAG sulfation density, and chain length.

Synthesis of Cluster-xylosides. We hypothesize that cluster-xylosides carrying multiple GAG chains per scaffold can better mimic PGs and therefore these scaffolds can be utilized to define the biological significance of GAG multivalency. Toward this goal, we designed a library of cluster-xylosides that can prime multiple GAG chains per scaffold and mimic naturally occurring PGs. A library of mono-xylosides synthesized by click chemistry has been found to be stable under *in*

vitro conditions and furthermore possesses good GAG priming activity.[16] Therefore, we employed click chemistry in our current study to synthesize mono-xylosides, bis-xylosides, tris-xylosides, and tetrakis-xylosides shown in Table 1.[25] Fully acetylated xylosyl azide was conjugated to various hydrophobic molecules containing triple bonds by click chemical methodology and the resulting library of xylosides was deprotected under Zemplén condition to obtain the final products as outlined in Scheme 1. The overall reaction yields of this two-step process, click chemistry and deprotection, range from 50% to 70%. The final products were purified on a reverse phase C18 column using HPLC as described in the Methods section followed by structural analysis using NMR spectroscopy and mass spectrometry.

Priming Activity of Cluster-xylosides. A mutant CHO cell line, pgsA-745, is a convenient cellular system for determining the priming activity of cluster-xylosides because this cell line lacks an active xylosyltransferase enzyme and therefore does not make endogenous GAG chains. Thus, it is straightforward to determine the priming activity of cluster-xylosides using this cell line. The priming activities of the protected and deprotected cluster-xylosides were compared (Supporting Information, Figure S1). Protected bis-xylosides (**3a** and **7a**) precipitated at higher concentrations (>250 μM). Therefore the priming activity of the bis-xylosides was analyzed using deprotected bis-xylosides. The deprotected bis-xylosides were screened at various concentrations, 100 μM, 300 μM, 600 μM, and 1 mM. The primed GAGs were purified using mini DEAE-sepharose columns. It is interesting to note that deprotected bis-xylosides were able to prime at these concentrations with a tendency to prime better with increasing concentration (Supporting Information, Figure S2). However, deprotected tris- and tetrakis-xylosides were unable to prime or poorly prime at any concentration, suggesting that these highly water-soluble scaffolds experience difficulties in crossing the

Table 1. Structures of Xylosides
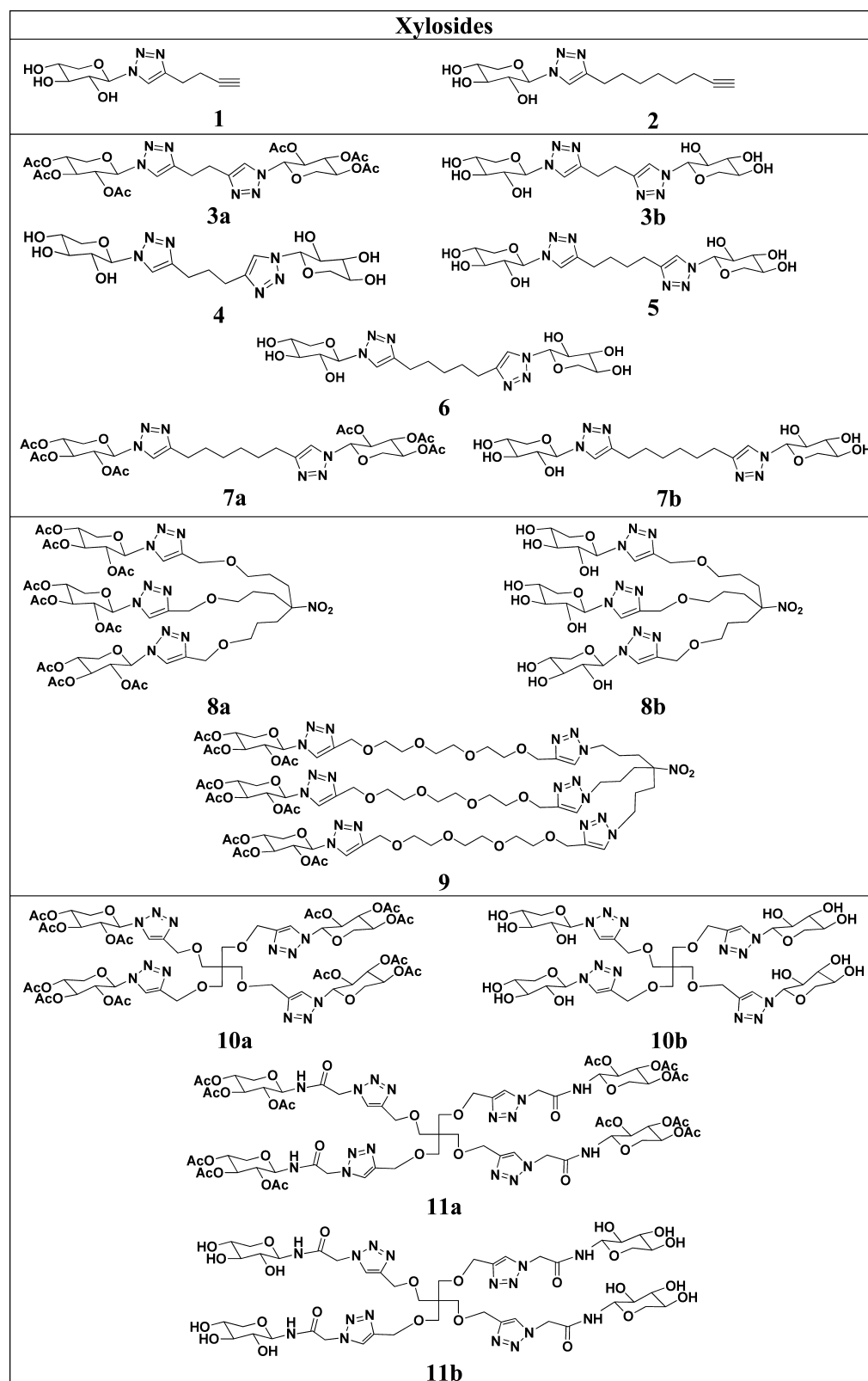
intracellular and/or outer membranes (Supporting Information, Figure S3). For these reasons, fully acetylated tris- and tetrakis-xylosides were studied for their priming activity. Fully protected cluster-xylosides (**8−11**) precipitated at 1 mM concentration in the cell culture medium, whereas these scaffolds were found to

prime GAG chains without getting precipitated at the 100 μM concentration in the cell culture medium. Next, we examined the effect of spacer length between xylose units on the priming activity. The obtained data shows that the distance between the xylose units located on a single scaffold affects the priming

Scheme 1. Synthesis of Cluster-xylosides[a]

n = 1, 2, 3, 4
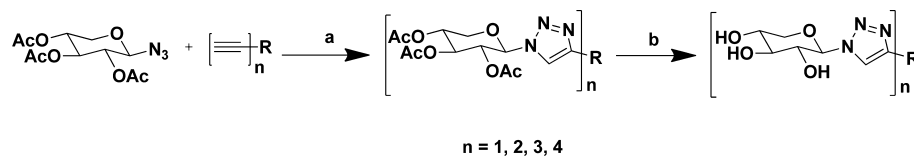
[a](a) Acetone, deionized water, copper(II) sulfate, and sodium ascorbate; (b) methanol and sodium methoxide.

activity at 100 μM concentration as shown in Figure 2. At the 100 μM concentration, as the spacer distance increases, the
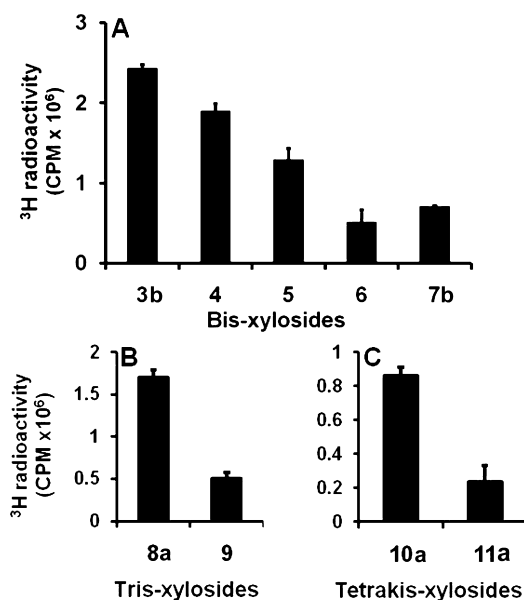
Figure 2. Priming activity of cluster-xylosides. Mutant CHO cells, pgsA-745, were treated with cluster-xylosides (100 μM concentration) in the presence of ^{3}H-GlcNH$_2$ (100 μCi) as described in the Methods section. The primed GAG chains were purified by anion-exchange chromatography and quantitated using a liquid scintillation counter. Priming activity of bis-xylosides (A), fully tris-xylosides (B), and fully tetrakis-xylosides (C) are shown. The results are the average of two independent experiments that were carried out in duplicate.

priming activity tends to decrease for all cluster-xylosides, suggesting that longer alkyl linkers may prohibit effective transport of cluster-xylosides across the membrane. For the majority of bis-xylosides, the spacer distance between the two xylose units did not have any effect on the priming activity at 1 mM (Supporting Information, Figure S4).

Structural Analysis of Primed GAG Chains. In order to verify the multidirectional priming ability of cluster-xylosides, we analyzed the molecular weights of GAG chains induced by cluster-xylosides in pgsA-745 cells using size exclusion chromatography. The chain length of the GAG chains was determined by measuring the migration time of GAG chains in comparison to that of polystyrene sulfonate standards under similar conditions (Supporting Information, Figure S5). The average molecular weights were found to be 16 KDa for GAG chains primed by mono-xyloside (**1**), 55 KDa for GAG chains primed by bis-xyloside (**3b**), 32 KDa for GAG chains primed by tris-xyloside (**8a**), and 40 KDa for GAG chains primed by tetrakis-xyloside (**10a**). The tris- and tetrakis-xylosides produced GAG chains with a higher average molecular weight than the mono-xylosides but lower molecular weight compared

to those produced by the bis-xylosides. This may possibly be due to molecular steric hindrance that decreased enzyme efficiency during GAG biosynthesis (Figure 3, panels A–C). Available data suggests that bis-xylosides prime GAG chains that have higher molecular weights and less polydispersity in comparison to those that are primed by tris- or tetrakis-xylosides. Though bis-xylosides prime better at 1 mM concentration compare to 100 μM concentration, primed GAG chains are lower in their molecular weights (Figure 3, panel D). This could be due to the overloading of GAG biosynthetic machinery with xylosides. We have also found that the spacer distance between the two residues in bis-xylosides did not affect average MWs of primed GAG chains even though the spacer distance affected their priming activity at 100 μM concentration.

High pressure DEAE anion-exchange chromatography was employed to compare the sulfation pattern of primed GAG chains. Interestingly, the average MWs of primed GAG chains are affected by the number of xylose units per scaffold, but on the basis of the elution time the sulfation density of various primed GAG chains was largely unaffected (Supporting Information, Table S1, Figure S6). The HS/CS composition of primed GAG chains was determined by treating them with heparitinases I/II/III or chondroitinase ABC (Supporting Information, Figure S7). It was found that these cluster-xylosides in this study predominantly prime CS chains and relatively smaller quantities of HS chains. Earlier studies, including our own, hasve shown that aglycone structures dramatically influence the GAG composition and that aglycones carrying naphthyl or aryl group tend to prime more HS chains. For these reasons, we synthesized additional bis-xyloside scaffolds in which phenyl or naphthyl group-containing linkers were used to bridge two xylose residues as shown in Table 2. In our later efforts, we primarily focused on synthesizing additional bis-xylosides as they tend to prime GAG chains with higher molecular weights and less polydispersity than tris- or tetrakis-xylosides. The additional scaffolds (**12–19**) were also found to prime GAG chains (Supporting Information, Figure S8). However, they primed mostly CS chains and very few HS chains even though they carry phenyl or naphthyl groups. Nevertheless, bis-xylosides should mimic PGs such as biglycan that carry two CS chains and therefore can be used as potential PG mimetics to define the GAG multivalency in the biological systems. Furthermore, it is possible that these scaffolds prime different GAG types in other cellular systems.

To determine the disaccharide composition, the purified GAG chains were treated with chondroitinase ABC that digests CS chains into disaccharides. The radiolabeled disaccharides were then identified by comparison of their elution positions relative to those of disaccharide standards. Disaccharide analysis revealed that primed CS chains composed of two major disaccharides, ΔUA-GalNAc (I) and ΔUA-GalNAc(4S) (II). GAG chains primed by the bis-xylosides (**3b** and **7b**) at 100 μM concentration were composed mostly of 4-O-sulfated
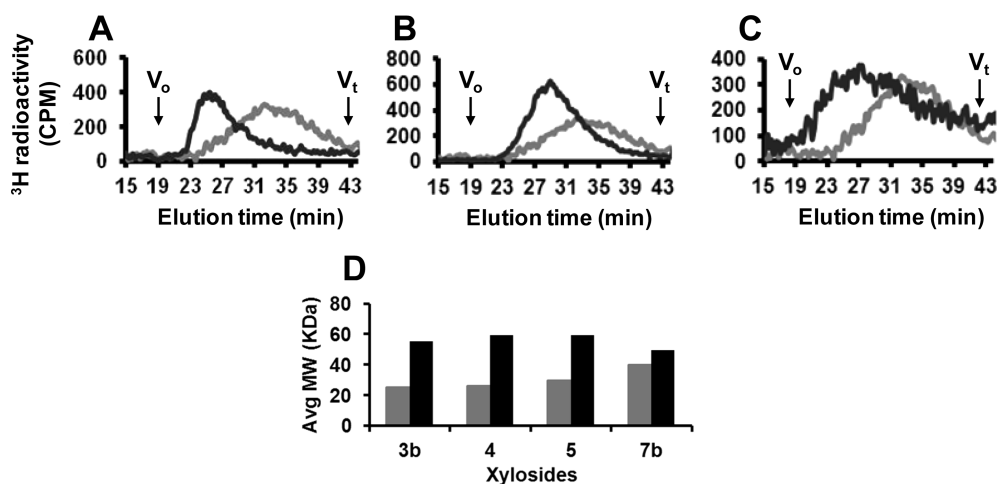
Figure 3. Structural analysis of primed GAG chains. Mutant CHO cells, pgsA-745, were treated with cluster-xylosides (100 μM concentration) for 24 h, and the primed GAG chains were purified as described in the Methods section. The purified GAG chains were analyzed by size exclusion chromatography as described in the Methods section. (A) The elution profiles of GAG chains primed by mono-xyloside (**1**) (gray trace, control) and bis-xyloside (**3b**) (black trace). (B) The elution profiles of GAG chains primed by mono-xyloside (**1**) (gray trace, control) and tris-xyloside (**8a**) (black trace). (C) The elution profiles of GAG chains primed by mono-xyloside (**1**) (gray trace, control) and tetrakis-xyloside (**10a**) (black trace). (D) Molecular weight analysis of GAG chains primed by bis-xylosides (**3b**, **4**, **5**, and **7b**) in the pgsA-745 cell line at 100 μM (black trace) and 1 mM (gray trace) concentrations.

disaccharide (Figure 4). Moreover, GAG chains primed by various cluster-xylosides at 100 μM concentration were composed mostly of 4-O-sulfated CS disaccharide (Supporting Information, Figure S9). This observation further supports our claim that the primed GAG chains have largely similar sulfation density (Supporting Information, Figure S6).

Evidence of Bidirectional Priming by Bis-xylosides. In order to confirm bidirectional priming of GAG chains by bis-xylosides, the GAG chains primed by mono-xylosides and bis-xylosides were subjected to periodate oxidation-alkaline elimination.[18] As expected, there are no changes in the MWs of GAG chains primed by mono-xylosides after treatment with periodate oxidation-alkaline elimination conditions (Supporting Information, Figure S10, panel A). However, the apparent MWs of bivalent GAG chains, primed by bis-xyloside **7**, changed from ~55 KDa to ~20 KDa, indicating that two covalently attached GAG chains were cleaved into two individual GAG chains. It is interesting to note that the apparent MW of the intact structure is higher than sum of the MWs of two individual GAG chains, suggesting differences in the hydrodynamic volume of individual chains when they are found in the attached or detached form (Supporting Information, Figure S10, panel B). GAG chains primed by tris- and tetrakis-xyloside scaffolds were not subjected to this oxidation-elimination condition, as these xylosides did not produce GAG scaffolds with proportional increase in the apparent MWs with increasing number of xylose units. In addition to oxidation-elimination technique to cleave the scaffold, we also devised another chemical strategy, ozonolysis, a milder technique, which selectively cleaves the scaffold carrying double bond. For this reason, we synthesized bis-xyloside **20** carrying alkenyl linker that can easily be cleaved under milder conditions using ozone reagent. When GAG chains primed by bis-xyloside **20** were subjected to ozone treatment, the primed scaffold was cleaved into two independent GAG chains (Supporting Information, Figure S11). Therefore, obtained data, from two independent techniques, unequivocally suggested that bis-xylosides primed
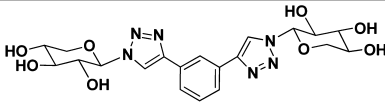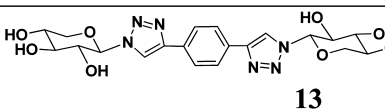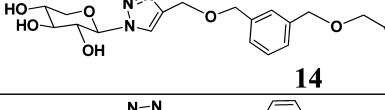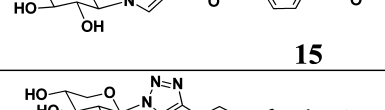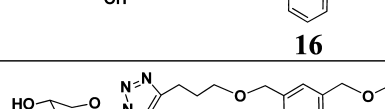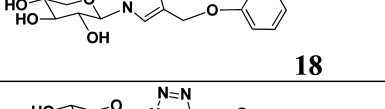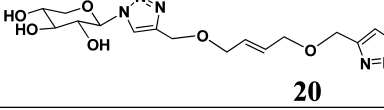
two GAG chains in a bidirectional manner leading to the production of scaffolds that mimic natural PGs.
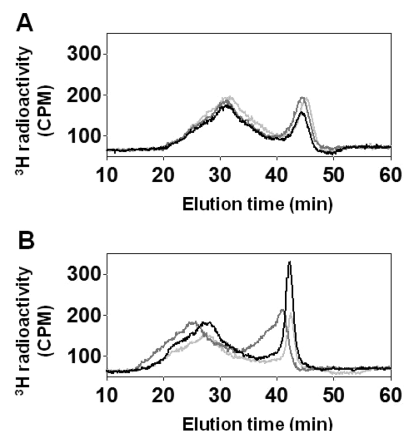
Effect of Cluster Xylosides on Endogenous GAG Chains. To determine the effects of cluster-xylosides on endogenous GAG chains, wild-type K1 CHO cells were treated with two bis-xylosides (**3b** and **7b**) at 100 μM and 1 mM concentrations for 24 h. The medium was removed, and CHO cells were then washed with PBS buffer. The endogenous GAGs were released from cell surface bound PGs by treating cells with Pronase and purified through a mini-DEAE column as described in Methods. The sulfation density of endogenous GAG was not affected at 100 μM, whereas at a very high concentration (1 mM), cluster-xylosides moderately affected the endogenous GAG chains (Figure 5).

Mechanism of Assembly of PGs. Lander et al. proposed a two-step biosynthetic model in which the decisions to attach CS or HS to a core protein are made sequentially.[26] If this were the case, one could expect to observe distinct GAG types primed at two different GAG initiation sites in these synthetic scaffolds. However, we did not observe the priming of two different GAG types. It is therefore tempting to propose an alternative model in which scaffolds reach specific GAGO-SOMES through their selective trafficking into the Golgi where they are committed for assembling either HS or CS/DS at multiple initiation sites as long as the initiation sites are in close proximity. However, the model proposed by Lander may very well be true if there are additional unknown factors that can recognize protein sequences and thereby facilitate the assembly mechanism in a two-step process that eventually leads to the production of PGs carrying both HS and CS/DS on the same core protein. Thus, the biosynthetic machinery cannot impose these molecular restrictions on cluster-xylosides as these scaffolds lack such elaborative structural features to facilitate the two-step process.

In summary, a wide variety of cluster-xylosides carrying two, three, or four xylose residues per scaffold were synthesized using click chemistry and systematically studied their ability to prime multivalent GAG chains in comparison to mono-

Table 2. Structures of Bis-xylosides Carrying an Aryl Group in the Aglycone

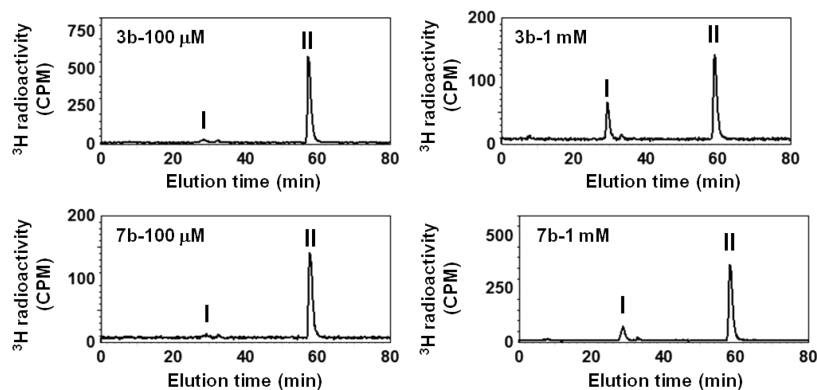| Xylosides |
|---|
| **12** |
| **13** |
| **14** |
| **15** |
| **16** |
| **17** |
| **18** |
| **19** |
| **20** |

Figure 5. Effect of bis-xylosides on endogenous GAG chains in wild type K1 CHO cells. K1 cells were treated with bis-xyloside (**3b** and **7b**) at 100 μM and 1 mM in the presence of ^{35}S-sulfate (100 μCi) as described in Methods. The endogenous GAG chains were purified, and their structures were analyzed using anion exchange HPLC. These elution profiles are representative of two independent experiments. (A) The elution profiles of endogenous GAG chains in control wells (light brown trace, control), in wells treated with 100 μM of bis-xyloside (**3b**) (dark brown trace) and in wells treated with 100 μM of bis-xyloside (**7b**) (black trace). (B) The elution profiles of endogenous GAG chains in control wells (light brown trace, control), in wells treated with 1 mM of bis-xyloside (**3b**) (dark brown trace), and in wells treated with 1 mM of bis-xyloside (**7b**) (black trace).

xylosides. Cluster-xylosides primed multiple GAG chains per scaffold, mimicking endogenous PGs. Most of these cluster-xylosides primed predominantly multivalent CS chains. These scaffolds will serve as excellent chemical biology tools to further understand the mechanism of assembly of multiple GAG chains as occurs in PGs for the first time and also to examine the biological significance of GAG multivalency in a systematic manner in model organisms. Future studies will focus on the synthesis of additional cluster-xylosides to understand the biosynthetic factors that differentially regulate the assembly of HS and CS chains

■ METHODS

Materials. The mutant Chinese hamster ovary (CHO) cell line, pgsA-745, was obtained from American Type Culture Collection. The cell culture reagents for the CHO cell line were obtained from HyClone. Tritium glucosamine (^{3}H) and Ultima-FloAP flow

Figure 4. Disaccharide profiles of bis-xyloside primed CS chains. GAG chains, which were primed by bis-xylosides (**3b** and **7b**) at 100 μM and 1 mM, were treated with chondroitinase ABC, and the resulting disaccharides were analyzed by SAX-HPLC. I, ΔUA-GalNAc; and II, ΔUA-GalNAc4S.

scintillation mixture for flow radiometric analysis were obtained from Perkin-Elmer Life Sciences. All other chemicals and biochemicals were obtained from Sigma Aldrich. DEAE-Sepharose gel was purchased from Amersham Biosciences. The anion-exchange column, TSKgel DEAE-3SW (7.4 mm × 7.5 cm), and the size exclusion column, G3000SWXL (7.8 mm × 30 cm), were obtained from Tosoh Bioscience. Anhydrous solvents were purchased and used directly or dried over standard drying agents and freshly distilled prior to use.

Synthesis of Cluster-xylosides. Propargylated precursors for the synthesis of cluster-xylosides (**8−11**, **14−17**, and **20**) were prepared as follows: Scaffolds, carrying multiple hydroxyl groups (1 mmol), were taken in a 100 mL RB flask, and dry tetrahydrofuran (20 mL) was added, followed by addition of sodium hydride (3 mmol). The reaction was carried out at RT for 30 min, followed by addition of propargyl bromide (3 mmol). The synthesis of cluster-xylosides **18** and **19** is described in the Supporting Information. Progress of the reaction was monitored by TLC using ethyl acetate and hexane as eluants. After the reaction was complete, the reaction mixture was evaporated using a rotary evaporator under reduced pressure. The reaction mixture was diluted with ethyl acetate. The organic layer was washed with water, dried over sodium sulfate, and further purified by silica flash column to give the propargylated molecules, which were then characterized by NMR spectroscopy and mass spectrometry. Tetra-*O*-propargyl pentaerythritol,[27] required for the synthesis of cluster-xylosides **10** and **11**, and *N*-(2,3,4-tri-*O*-acetyl-*β*-D-xylopyranosyl) azidoacetamide,[27] needed for the synthesis of cluster-xyloside **11** were prepared following the literature procedure.

Next, to a solution of propargylated precursors (1 mmol) and xylosyl azide (1, 2, 3, or 4 mmol for the synthesis of mono-, bis-, tris-, or tetrakis-xylosides, respectively) in an acetone (8 mL) and water (2.6 mL) mixture was added excess sodium ascorbate, followed by CuSO$_4$·5H$_2$O (0.4 mmol) at RT, and the mixture was stirred until the disappearance of the starting materials, as indicated by TLC. At the end of the reaction, the reaction mixture was concentrated using a rotary evaporator under reduced pressure, and the syrup obtained was dissolved in ethyl acetate and washed with water. Finally, the organic layers were washed with saturated sodium chloride, and the crude products were purified by silica flash column to give the desired protected xylosides. Deprotection procedure: Fully acetylated xyloside (1 mmol) was taken in dry methanol (10 mL) and treated with freshly prepared 1 M solution of sodium methoxide in dry methanol until the solution reached pH ∼9 as indicated by pH paper. After the deacetylation was complete as indicated by TLC, H$^+$ resins were added to bring the pH to 7. The reaction mixture was then filtered, concentrated under reduced pressure to the crude product, and further purified on HPLC-reverse phase C18 column with solvent A (25 mM formic acid in water) and solvent B (95% acetonitrile) to give the deprotected-xylosides (**1−20**).

Xyloside 1. ^{1}H NMR (CD$_3$OD) δ 7.98 (1H, s, triazolyl H), 5.47 (1H, d, *J* = 9.4 Hz, H-1), 4.00 (1H, dd, *J* = 5.1, 11.3 Hz, H-5a), 3.87 (1H, t, *J* = 9.4 Hz, H-2), 3.67−3.63 (1H, m, H-4), 3.49 (1H, t, *J* = 9.0 Hz, H-3), 3.45 (1H, t, *J* = 10.9 Hz, H-5b), 2.92 (2H, t, *J* = 7.4 Hz,), 2.54 (2H, dt, *J* = 2.3 Hz, 7.4 Hz), 2.27 (1H, t, *J* = 2.7 Hz); ^{13}C NMR (CD$_3$OD) δ 147.4, 122.7, 90.2, 83.8, 78.6, 73.9, 70.7, 70.5, 69.8, 25.9, 19.3; ESI-MS calcd for C$_{11}$H$_{15}$N$_3$O$_4$Na 276.0960 [M + Na]$^+$, found 275.9333.

Xyloside 2. ^{1}H NMR (CD$_3$OD) δ 7.89 (1H, s, triazolyl H), 5.45 (1H, d, *J* = 9.4 Hz, H-1), 4.00 (1H, dd, *J* = 5.1, 11.1 Hz, H-5a), 3.87 (1H, t, *J* = 9.4 Hz, H-2), 3.69−3.63 (1H, m, H-4), 3.48 (1H, t, *J* = 9.4 Hz, H-3), 3.45 (1H, t, *J* = 10.9 Hz, H-5b), 2.71 (2H, t, *J* = 7.8 Hz,), 2.17−2.14 (3H, m), 1.72−1.65 (2H, m), 1.52−1.36 (6H, m); ^{13}C NMR (CD$_3$OD) δ 149.2, 122.2, 90.1, 85.0, 78.7, 73.8, 70.7, 69.8, 69.5, 30.4, 29.7, 29.6, 29.5, 26.2, 19.0; ESI-MS calcd for C$_{30}$H$_{46}$N$_6$O$_8$Na 641.3275 [2M + Na]$^+$, found 640.7333.

Xyloside 3a. ^{1}H NMR (CDCl$_3$) δ 7.44 (2H, s, triazolyl, H), 5.73 (2H, d, *J* = 8.59 Hz, H-1), 5.44−5.35 (4H, m, H-2, H-3), 5.15−5.09 (2H, m, H-4), 4.22 (2H, dd, *J* = 5.9 and 11.5 Hz, H-5a), 3.56 (2H, t, *J* = 11.3 Hz, H-5b), 2.68 (4H, t, *J* = 7.42 Hz), 2.05−2.04 (12H, m, 4xCOCH$_3$ each), 1.84 (6H, s, 2 × COC$\underline{H}_3$ each), 1.63 (4H, m), 1.31 (4H, m); ^{13}C NMR (CDCl$_3$) δ 169.8, 169.6, 169.3, 147.1, 119.7, 86.3,

72.1, 70.6, 68.0, 65.5, 25.3, 20.6, 20.4, 20.2; ESI-MS calcd for C$_{28}$H$_{36}$N$_6$O$_{14}$Na 703.2187 [M + Na]$^+$, found 703.0667

Xyloside 3b. ^{1}H NMR (CD$_3$OD) δ 7.84 (2H, s, triazolyl H), 5.45 (2H, d, *J* = 9.4 Hz, H-1), 3.99 (2H, dd, *J* = 5.5, 11.3 Hz, H-5a), 3.83 (2H, t, *J* = 9.4 Hz, H-2), 3.69−3.63 (2H, m, H-4), 3.48 (2H, t, *J* = 9.0 Hz, H-3), 3.44 (2H, t, *J* = 10.9 Hz, H-5b), 3.09 (4H, s); ^{13}C NMR (CD$_3$OD) δ 169.0, 122.7, 90.2, 78.6, 74.0, 70.7, 69.8, 26.2; ESI-MS calcd for C$_{16}$H$_{24}$N$_6$O$_8$Na 451.1553 [M + Na]$^+$, found 451.1333.

Xyloside 4. ^{1}H NMR (CD$_3$OD) δ 7.94 (2H, s, triazolyl H), 5.46 (2H, d, *J* = 9.4 Hz, H-1), 3.99 (2H, dd, *J* = 5.5, 11.3 Hz, H-5a), 3.87(2H, t, *J* = 9.4 Hz, H-2), 3.70−3.64 (2H, m, H-4), 3.49 (2H, t, *J* = 9.0 Hz, H-3), 3.45 (2H, t, *J* = 10.9 Hz, H-5b), 2.76 (4H, t, *J* = 7.4 Hz), 2.05 (2H, p, *J* = 7.4 Hz); ^{13}C NMR (CD$_3$OD) δ 148.4, 122.5, 90.2, 78.6, 73.9, 70.7, 69.8, 29.9, 25.5; ESI-MS calcd for C$_{17}$H$_{27}$N$_6$O$_8$ 443.1890 [M + H]$^+$, found 442.8667.

Xyloside 5. ^{1}H NMR (CD$_3$OD) δ 7.89 (2H, s, triazolyl H), 5.45 (2H, d, *J* = 9.4 Hz, H-1), 3.99 (2H, dd, *J* = 5.1, 11.1 Hz, H-5a), 3.86 (2H, t, *J* = 9.4 Hz, H-2), 3.69−3.63 (2H, m, H-4), 3.48 (2H, t, *J* = 9.0 Hz, H-3), 3.45 (2H, t, *J* = 11.3 Hz, H-5b), 2.74 (4H, t, *J* = 6.6 Hz), 1.75−1.72 (4H, m); ^{13}C NMR (CD3OD) δ 148.9, 122.3, 90.2, 78.7, 73.9, 70.7, 69.8, 29.7, 25.9; ESI-MS calcd for C$_{18}$H$_{29}$N$_6$O$_8$ 457.2047 [M + H]$^+$, found 457.0450.

Xyloside 6. ^{1}H NMR (CD$_3$OD) δ 7.89 (2H, s, triazolyl H), 5.46 (2H, d, *J* = 9.4 Hz, H-1), 4.00 (2H, dd, *J* = 5.5, 11.3 Hz, H-5a), 3.87(2H, t, *J* = 9.4 Hz, H-2), 3.70−3.64 (2H, m, H-4), 3.49 (2H, t, *J* = 9.0 Hz, H-3), 3.45 (2H, t, *J* = 11.3 Hz, H-5b), 2.71 (4H, t, *J* = 7.8 Hz), 1.75−1.68 (4H, m), 1.42 (2H, p, *J* = 7.8 Hz); ^{13}C NMR (CD$_3$OD) δ 149.1, 122.3, 90.1, 78.7, 73.9, 70.7, 69.8, 30.0, 29.5, 26.1; ESI-MS calcd for C$_{19}$H$_{31}$N$_6$O$_8$ 471.2203 [M + H]$^+$, found 471.0000.

Xyloside 7a. ^{1}H NMR (CDCl$_3$) δ 7.53 (2H, s, triazolyl, H), 5.74 (2H, d, *J* = 8.2 Hz, H-1), 5.42−5.35 (4H, m, H-2, H-3), 5.17−5.11 (2H, m, H-4), 4.26 (2H, dd, *J* = 5.9 and 11.5 Hz, H-5a), 3.56 (2H, t, *J* = 10.9 Hz, H-5b), 3.14 (2H, d, *J* = 9.38 Hz), 2.94 (2H, d, *J* = 9.4 Hz), 2.02, 1.90 (18H, s, 6 × COC$\underline{H}_3$ each). ^{13}C NMR (CDCl$_3$) δ 169.9, 169.7, 169.0, 149.0, 118.7, 86.2, 72.1, 70.3, 68.4, 65.5, 28.8, 28.6, 25.4, 20.6, 20.5. 20.1; ESI-MS calcd for C$_{32}$H$_{44}$N$_6$O$_{14}$Na 759.2813 [M + Na]$^+$, found 759.0667

Xyloside 7b. ^{1}H NMR (CD$_3$OD) δ 7.89 (2H, s, triazolyl H), 5.45 (2H, d, *J* = 9.4 Hz, H-1), 3.99 (2H, dd, *J* = 5.1, 11.3 Hz, H-5a), 3.87 (2H, t, *J* = 9.0 Hz, H-2), 3.70−3.63 (2H, m, H-4), 3.48 (2H, t, *J* = 9.0 Hz, H-3), 3.45 (2H, t, *J* = 11.3 Hz, H-5b), 2.69 (4H, t, *J* = 7.4 Hz), 1.70−1.66 (4H, m), 1.41−1.38 (4H, m); ^{13}C NMR (CD$_3$OD) δ 149.2, 122.3, 90.1, 78.7, 73.9, 70.7, 69.8, 30.2, 29.8, 26.1; ESI-MS calcd for C$_{20}$H$_{32}$N$_6$O$_8$Na 507.2179 [M + Na]$^+$, found 507.2050.

Xyloside 8a. ^{1}H NMR (CDCl$_3$) δ 7.78 (3H, s, triazolyl H), 5.80 (3H, d, *J* = 9.0 Hz, H-1), 5.44−5.38 (6H, m, H-2, H-3), 5.20−5.14 (3H, m, H-4), 4.59 (6H, s), 4.29 (3H, dd, *J* = 5.5, 11.5 Hz, H5-a), 3.60 (3H, t, *J* = 11.3 Hz, H-5b); 3.45 (6H, t, *J* = 5.9 Hz), 2.07 (9H, s, Ac-H), 2.05 (9H, s, Ac-H), 1.98−1.94 (6H, m), 1.86 (9H, s, Ac-H), 1.51−1.44 (6H, m); ESI-MS calcd for C$_{52}$H$_{72}$N$_{10}$O$_{26}$Na 1275.4517 [M + Na]$^+$, found 1275.2039.

Xyloside 8b. ^{1}H NMR (CD$_3$OD) δ 8.13 (1H, s, triazolyl-H), 5.51 (1H, d, *J* = 9.4 Hz, H-1), 4.57 (2H, s), 4.00 (1H, dd, *J* = 5.5, 11.3 Hz, H-5a), 3.90 (1H, t, *J* = 9.0 Hz, H-2), 3.71−3.65 (1H, m, H-4), 3.50 (1H, t, *J* = 9.0 Hz, H-3), 3.46 (1H, t, *J* = 10.6 Hz, H-5b), 3.49 (2H, t, *J* = 11.3 Hz), 1.93−1.97 (2H, m), 1.48−1.41(2H, m); ^{13}C NMR (CD$_3$OD): 144.9, 123.0, 94.2, 89.0, 77.4, 72.7, 69.7, 69.5, 68.7, 63.4, 32.1, 23.8; ESI-MS calcd for C$_{34}$H$_{55}$N$_{10}$O$_{17}$ 875.3747 [M + H]$^+$, found 875.1756.

Xyloside 9. ^{1}H NMR (MeOD) δ 8.23 (3H, s, triazolyl H), 7.97 (3H, s, triazolyl H), 6.02 (3H, d, *J* = 9.0 Hz, H-1), 5.57 (3H, t, *J* = 9.4 Hz, H-2), 5.49 (3H, t, *J* = 9.4 Hz, H-3), 5.23−5.163 (3H, m, H-4), 4.64 (6H, s), 4.62 (6H, s), 4.37 (6H, t, *J* = 6.6 Hz), 4.23 (3H, dd, *J* = 5.5 Hz, 11.5 Hz, H-5a), 3.76 (3H, t, *J* = 10.9 Hz, H-5b), 3.64−3.59 (36H, m), 2.04 (9H, s, 3 × COC$\underline{H}_3$), 2.01 (9H, s, 3 × COC$\underline{H}_3$), 1.89−1.84 (6H, m), 1.82 (9H, s, 3 × COC$\underline{H}_3$), 1.65 (6H, m); ^{3}C NMR (CD$_3$OD) δ 171.5, 171.5, 170.5, 146.7, 125.4, 124.2, 94.4, 87.2, 73.8, 72.0, 71.5, 71.5, 70.8, 70.7, 69.8, 66.2, 65.0, 64.8, 50.7, 33.0, 25.4, 20.6, 20.6, 20.2. ESI-MS calcd for C$_{79}$H$_{117}$N$_{19}$O$_{35}$Na 1914.7857 [M + Na]$^+$, found 1914.4667.

Xyloside 10a. ^{1}H NMR (CDCl$_3$) δ 7.94 (4H, s, triazolyl, H), 5.89 (4H, d, J = 9.2 Hz, H-1), 5.51 (4H, t, J = 9.2 Hz, H-2), 5.45 (4H, t, J = 9.2 Hz, H-3), 5.26 (4H, m, H-4), 4.62 and 4.54 (4H each, ABq, Ar-CH$_2$O-), 4.29 (4H, dd, J = 5.6 and 11.6 Hz, H-5a), 3.66 (4H, M, H-5b), 3.42 (8H, s, -OCH$_2$-C), 2.09, 2.07, 1.83 (36H, s, 12 × COCH$_3$ each); ^{13}C NMR (CDCl$_3$) δ 170.0, 169.8, 169.0 (4 × -COCH$_3$ each), 146.0, 121.4, 86.2 (C-1), 72.4, 70.6, 69.2, 68.6, 65.5, 64.8, 45.2 (core carbon), 20.7, 20.6, 20.1 (4 × COCH$_3$ each); ESI-MS calcd for C$_{61}$H$_{81}$N$_{12}$O$_{32}$ 1493.5080 [M + H]$^+$, found 1493.5043.

Xyloside 10b. ^{1}H NMR (400 MHz, CDCl$_3$) δ 8.13 (s, 4H), 5.62 (d, 4H, J = 8.8 Hz, H-1), 4.51 (s, 8H, CH$_2$), 4.09 (dd, 4H, J = 5.4 and 11.4 Hz, H-5a), 3.98 (t, 4H, J = 9.2 Hz, H-2), 3.80 (m, 4H, H-4), 3.64 (t, 4H, J = 9.2 Hz, H-3), 3.55 (t, 4H, J = 11.2 Hz, H-5b), 3.36 (s, 8H, CH$_2$); ^{13}C NMR (100 MHz, CDCl$_3$) δ 147.0, 126.8, 90.9 (C-1), 79.3, 75.1, 71.5, 70.9, 70.8, 66.1, 47.1; ESI-MS calcd for C$_{37}$H$_{56}$N$_{12}$O$_{20}$Na 1011.3632 [M + Na]$^+$, found 1011.3630.

Xyloside 11a. ^{1}H NMR (CDCl$_3$) δ 7.72 (4H, s, triazolyl, H), 7.70 (4H, d, br, 4 × -NH), 5.24–5.34 (8H, m, H-3 and H-1), 5.12 and 5.04 (4H each, ABq, -COCH$_2$N), 5.03–4.90 (8H, m, H-2 and H-4), 4.53 (8H, s, Ar-CH$_2$O-), 4.09 (4H, m, H-5a), 3.46 (4H, m, H-5b), 3.40 (8H, s, -OCH$_2$-C), 2.04 (36H, s, -COCH$_3$); ^{13}C NMR (CDCl$_3$) δ 170.7, 169.9, 169.8 (4 × COCH$_3$ each), 166.7 (4 × -NHCO-), 145.4, 124.5, 78.7 (C-1), 72.5, 70.5, 68.8 (2 × C), 67.1, 64.5 (C-5), 52.4 (-COCH$_2$-), 45.1 (core carbon), 20.6–20.5 (3 × C, 4 × -COCH$_3$ each); ESI-MS calcd for C$_{69}$H$_{94}$N$_{16}$O$_{36}$ 861.3009 [M + 2H]$^{2+}$, found 861.3010.

Xyloside 11b. ^{1}H NMR (400 MHz, CDCl$_3$) δ 7.96 (s, 4H), 4.93 (d, 4H, J = 8.8 Hz, H-1), 4.52 (s, 8H, CH$_2$), 3.92 (dd, 4H, J = 5.6 and 11.2 Hz, H-5a), 3.62 (m, 4H, H-4), 3.49 (t, 4H, J = 9.2 Hz, H-3), 3.45–3.34 (m, 16H, H-2, H-5b, CH$_2$ and CH$_2$); ^{13}C NMR (100 MHz, CDCl$_3$) δ 171.5 (-NHCO-), 147.1, 129.0, 82.5 (C-1), 79.2, 74.4, 71.7, 70.9, 69.6, 66.1, 51.6, 47.1; ESI-MS calcd for C$_{45}$H$_{69}$N$_{16}$O$_{24}$: 1217.4671 [M + H]$^+$, found 1217.4717.

Screening of Cluster-xylosides in CHO Cells. To determine whether cluster-xylosides were able to prime GAG chains, the cells were treated with cluster-xylosides at 100 μM or 1 mM concentration in the presence of ^{3}H-glucosamine. Primed GAGs were purified and analyzed as described below. Cells (4 × 10^5 per well) were seeded in complete growth medium in a 6-well plate. The cells were incubated at 37 °C in a humidified incubator for 24 h to 50% confluency. The cells were then washed with sterile PBS and replaced with 990 μL of DMEM containing 10% dialyzed FBS and 1 mM of glucose. A solution containing a specific primer at 100X the final concentration was prepared. Ten microliters of appropriate 100X primer stock was added to various wells to achieve an appropriate concentration. 100 μCi of ^{3}H-glucosamine was also added to each well as tracer. The 6 well plates were incubated at 37 °C in a humidified incubator (5% CO$_2$) for 24 h.

Purification and Quantitation of GAG Chains. The entire content of each well was transferred to a microcentrifuge tube and subjected to centrifugation at 16000xg for 5 min. The supernatant was transferred to a fresh tube and 0.016% Triton X-100 (1.5 volumes) was added. The diluted supernatant was loaded on 0.2 mL DEAE-sepharose column pre-equilibrated with 2 mL of wash buffer (20 mM NaOAc, 0.1 M NaCl and 0.01% Triton X-100, pH 6.0) and the column was washed with 6 mL of wash buffer. The bound HS/CS was eluted with 1.2 mL of elution buffer (20 mM NaOAc and 1 M NaCl, pH 6.0). The priming activity of cluster-xylosides was evaluated by measuring the ^{3}H-radioactivity incorporated into the purified GAG chains using liquid scintillation counter.

Anion-Exchange HPLC Analysis. The purified GAG chains were analyzed by HPLC with an inline radiometric detector. Xyloside primed GAG chains of equal quantity were diluted 5-fold with HPLC solvent A (10 mM KH$_2$PO$_4$, pH 6.0, 0.2% CHAPS) for anion-exchange chromatography analysis. The sample was loaded on HPLC-DEAE column and eluted from the column with a linear gradient of 0.2 M to 1 M NaCl over 80 min at a flow rate of 1 mL/min. The radiolabeled GAG chains were detected by a radiometric flo-one A505A detector. The HPLC effluent was mixed with Ultima-Flo AP

scintillation cocktail at 1:2 ratio and detected in the flow scintillation analyzer.

Size-Exclusion HPLC Analysis. The chain length of the GAG chains synthesized by various cluster-xylosides was determined by measuring the migration time on two tandem G3000SWXL (Tosoh, 7.8 mm × 30 cm) size exclusion columns using the HPLC Hitachi system with an inline radiodetector. The solvent containing phosphate (100 mM KH$_2$PO$_4$, 100 mM NaCl, pH 6) was used as an eluent. The average molecular weight was determined by measuring the migration time of GAG chains in comparison to those of polystyrene sulfonate standards examined under similar conditions.

Compositional Analysis. The HS/CS composition of the primed GAG chains was determined by digesting the GAG chains with heparitinase I/II/III or chondroitinase ABC enzymes. The solution containing GAGs was diluted to 0.2 M NaCl, followed by the addition of heparitinase or chondroitinase ABC buffer and 5 mU of heparitinase I/II/III or chondroitinase ABC enzyme. The reaction mixture was incubated at 37 °C for 2 h, the solution was then loaded on to two tandem G3000 SWXL columns (7.8 mm × 30 cm) and analyzed with the aid of an inline radiometric detector using phosphate buffer (100 mM KH$_2$PO$_4$, 100 mM NaCl, pH 6) as an eluent. The percentage of HS/CS was determined based on the percentage area of undigested and digested GAG peaks.

Disaccharide Analysis. The disaccharide composition of CS chains was determined by digesting the GAG chains with chondroitinase ABC enzymes. The enzyme treated GAG mixture was analyzed using SAX-HPLC. CS disaccharide standards, ΔUA-GalNAc, ΔUA-GalNAc4S and ΔUA-GalNAc6S, were coinjected with enzyme digested GAG chains to deduce the disaccharide composition of primed GAG chains. The sample was eluted from the column with a linear gradient of 0 to 0.18 M NaCl over 100 min at a flow rate of 0.5 mL/min. The radiolabeled disaccharides were detected by a radiometric flo-one A505A detector. The HPLC effluent was mixed with Ultima-Flo AP scintillation cocktail at 1:2 ratio and detected in the flow scintillation analyzer.

Cleavage of Multiple GAG Chains into Individual GAG Chains. Mono- and bis- xyloside primed GAG chains were subjected to periodate oxidation using 0.02 M NaIO$_4$, 0.1 M sodium formate, pH 4.0 at 4 °C for 30 min. The reaction was stopped by addition of 0.04 M mannitol. The samples were desalted using 3000 cutoff membrane columns and subjected to alkali treatment with 0.1 M NaOH at pH 12 at 4 °C for 5 min.[18] GAG chains primed by bis-xyloside **20** were subjected to ozonolysis using ozone solution for 30 min, and resulting GAG chains were analyzed by size exclusion chromatography.

ASSOCIATED CONTENT

ⓈSupporting Information

This material is available free of charge via the Internet at http://pubs.acs.org.

AUTHOR INFORMATION

Corresponding Author

*E-mail: kuby@pharm.utah.edu; loganath@iitm.ac.in.

Notes

The authors declare no competing financial interest.

■ REFERENCES

(1) Perrimon, N., and Bernfield, M. (2000) Specificities of heparan sulphate proteoglycans in developmental processes. *Nature 404*, 725–728.

(2) Bernfield, M., Gotte, M., Park, P. W., Reizes, O., Fitzgerald, M. L., Lincecum, J., and Zako, M. (1999) Functions of cell surface heparan sulfate proteoglycans. *Annu. Rev. Biochem. 68*, 729–777.

(3) Raman, K., and Kuberan, B. (2010) Chemical tumor biology of heparan sulfate proteoglycans. *Curr. Chem. Biol. 4*, 20–31.

(4) Langford, J. K., Stanley, M. J., Cao, D., and Sanderson, R. D. (1998) Multiple heparan sulfate chains are required for optimal syndecan-1 function. *J. Biol. Chem. 273*, 29965–29971.

(5) Zhang, L., and Esko, J. D. (1994) Amino acid determinants that drive heparan sulfate assembly in a proteoglycan. *J. Biol. Chem. 269*, 19295–19299.

(6) Gopal, S., Bober, A., Whiteford, J. R., Multhaupt, H. A., Yoneda, A., and Couchman, J. R. (2010) Heparan sulfate chain valency controls syndecan-4 function in cell adhesion. *J. Biol. Chem. 285*, 14247–14258.

(7) Sanderson, R. D., and Bernfield, M. (1988) Molecular polymorphism of a cell surface proteoglycan: distinct structures on simple and stratified epithelia. *Proc. Natl. Acad. Sci. U.S.A. 85*, 9562–9566.

(8) Gotting, C., Kuhn, J., and Kleesiek, K. (2007) Human xylosyltransferases in health and disease. *Cell. Mol. Life. Sci. 64*, 1498–1517.

(9) Gotting, C., Muller, S., Schottler, M., Schon, S., Prante, C., Brinkmann, T., Kuhn, J., and Kleesiek, K. (2004) Analysis of the DXD motifs in human xylosyltransferase I required for enzyme activity. *J. Biol. Chem. 279*, 42566–42573.

(10) Schon, S., Prante, C., Bahr, C., Kuhn, J., Kleesiek, K., and Gotting, C. (2006) Cloning and recombinant expression of active full-length xylosyltransferase I (XT-I) and characterization of subcellular localization of XT-I and XT-II. *J. Biol. Chem. 281*, 14224–14231.

(11) Okayama, M., Kimata, K., and Suzuki, S. (1973) The influence of p-nitrophenyl beta-d-xyloside on the synthesis of proteochondroitin sulfate by slices of embryonic chick cartilage. *J. Biochem. 74*, 1069–1073.

(12) Galligani, L., Hopwood, J., Schwartz, N. B., and Dorfman, A. (1975) Stimulation of synthesis of free chondroitin sulfate chains by beta-D-xylosides in cultured cells. *J. Biol. Chem. 250*, 5400–5406.

(13) Schwartz, N. B. (1977) Regulation of chondroitin sulfate synthesis. Effect of beta-xylosides on synthesis of chondroitin sulfate proteoglycan, chondroitin sulfate chains, and core protein. *J. Biol. Chem. 252*, 6316–6321.

(14) Lugemwa, F. N., and Esko, J. D. (1991) Estradiol beta-D-xyloside, an efficient primer for heparan sulfate biosynthesis. *J. Biol. Chem. 266*, 6674–6677.

(15) Mani, K., Belting, M., Ellervik, U., Falk, N., Svensson, G., Sandgren, S., Cheng, F., and Fransson, L. A. (2004) Tumor attenuation by 2(6-hydroxynaphthyl)-beta-D-xylopyranoside requires priming of heparan sulfate and nuclear targeting of the products. *Glycobiology 14*, 387–397.

(16) Kuberan, B., Ethirajan, M., Victor, X. V., Tran, V., Nguyen, K., and Do, A. (2008) "Click" xylosides initiate glycosaminoglycan biosynthesis in a mammalian cell line. *ChemBioChem 9*, 198–200.

(17) Victor, X. V., Nguyen, T. K., Ethirajan, M., Tran, V. M., Nguyen, K. V., and Kuberan, B. (2009) Investigating the elusive mechanism of glycosaminoglycan biosynthesis. *J. Biol. Chem. 284*, 25842–25853.

(18) Johnsson, R., Mani, K., and Ellervik, U. (2007) Synthesis and biology of bis-xylosylated dihydroxynaphthalenes. *Bioorg. Med. Chem. 15*, 2868–2877.

(19) Esko, J. D., Stewart, T. E., and Taylor, W. H. (1985) Animal cell mutants defective in glycosaminoglycan biosynthesis. *Proc. Natl. Acad. Sci. U.S.A. 82*, 3197–3201.

(20) Kirn-Safran, C., Farach-Carson, M. C., and Carson, D. D. (2009) Multifunctionality of extracellular and cell surface heparan sulfate proteoglycans. *Cell. Mol. Life. Sci. 66*, 3421–3434.

(21) de Paz, J. L., Noti, C., Bohm, F., Werner, S., and Seeberger, P. H. (2007) Potentiation of fibroblast growth factor activity by synthetic heparin oligosaccharide glycodendrimers. *Chem. Biol. 14*, 879–887.

(22) Sasisekharan, R., and Venkataraman, G. (2000) Heparin and heparan sulfate: biosynthesis, structure and function. *Curr. Opin. Chem. Biol. 4*, 626–631.

(23) Esko, J. D., and Selleck, S. B. (2002) Order out of chaos: assembly of ligand binding sites in heparan sulfate. *Annu. Rev. Biochem. 71*, 435–471.

(24) Presto, J., Thuveson, M., Carlsson, P., Busse, M., Wilen, M., Eriksson, I., Kusche-Gullberg, M., and Kjellen, L. (2008) Heparan sulfate biosynthesis enzymes EXT1 and EXT2 affect NDST1 expression and heparan sulfate sulfation. *Proc. Natl. Acad. Sci. U.S.A. 105*, 4751–4756.

(25) Meldal, M., and Tornoe, C. W. (2008) Cu-catalyzed azide-alkyne cycloaddition. *Chem. Rev. 108*, 2952–3015.

(26) Chen, R. L., and Lander, A. D. (2001) Mechanisms underlying preferential assembly of heparan sulfate on glypican-1. *J. Biol. Chem. 276*, 7507–7517.

(27) Aich, U., and Loganathan, D. (2005) Synthesis of N-(beta-glycopyranosyl)azidoacetamides. *J. Carbohydr. Chem. 24*, 1–12.